Simultaneous Capturing of RGB and Additional Band Images Using Hybrid Color Filter Array

Daisuke Kiku, Yusuke Monno, Masayuki Tanaka, and Masatoshi Okutomi

Tokyo Institute of Technology

ABSTRACT

Extra band information in addition to the RGB, such as the near-infrared (NIR) and the ultra-violet, is valuable for many applications. In this paper, we propose a novel color filter array (CFA), which we call "hybrid CFA," and a demosaicking algorithm for the simultaneous capturing of the RGB and the additional band images. Our proposed hybrid CFA and demosaicking algorithm do not rely on any specific correlation between the RGB and the additional band. Therefore, the additional band can be arbitrarily decided by users. Experimental results demonstrate that our proposed demosaicking algorithm with the proposed hybrid CFA can provide the additional band image while keeping the RGB image almost the same quality as the image acquired by using the standard Bayer CFA.

Keywords: Demosaicking, color filter array (CFA), near-infrared (NIR) image.

1. INTRODUCTION

Extra band information in addition to the RGB such as the near-infrared (NIR), the ultra-violet, and a narrow-band is valuable for many applications, e.g., biometrics and medical imaging.[1,2] Recently, it is also reported that the joint use of the RGB and the additional band images improves the performance of the computer vision applications.[3–5]

One approach for capturing both the RGB and the additional band images is to sequentially capture the two images. However, this approach is not suitable for capturing a video due to the motion in the scene or from the camera between the two successive images. Another approach is to use a beam-splitter and two cameras, one is for the RGB and the other is for the additional band.[6] However, this approach is expensive since the setup is bulky.

On the other hand, a single sensor technology with a color filter array (CFA) and a demosaicking algorithm has advantages of low cost and exact alignment between the RGB and the additional band images.[7] Lu et al. and Sadeghipoor et al. respectively proposed a CFA and a demosaicking algorithm for the simultaneous capturing of the RGB and the NIR images.[8,9] These CFAs and demosaicking algorithms[8,9] are developed assuming strong correlation between the RGB and the NIR images. However, this assumption is not always true, which yields severe artifacts in uncorrelated regions. For this reason, we independently interpolate the RGB and the additional band images without assuming the specific correlation.

In this paper, we propose a novel color filter array (CFA), which we call "hybrid CFA," and a demosaicking algorithm for the simultaneous capturing of the RGB and the additional band images with the hybrid CFA. The proposed hybrid CFA is designed based on the most popular Bayer CFA,[10] so that an interpolation techniques for the Bayer CFA can be inherited. However, the demosaicking algorithms for the Bayer CFA cannot be directly applicable to the proposed hybrid CFA. Therefore, we propose a novel demosaicking algorithm for the hybrid CFA. The proposed demosaicking algorithm independently interpolates the RGB image and the additional band image, assuming that the additional band image is uncorrelated with the RGB image. For the RGB image demosaicking, we extend a state-of-the-art Bayer demosaicking algorithm to fit the proposed hybrid CFA. For the additional band image demosaicking, we apply a single-image super-resolution (SR) algorithm to effectively interpolate the missing additional band pixel values. Experimental results demonstrate that our proposed hybrid CFA and demosaicking algorithm can simultaneously acquire the high-quality RGB and the additional band images.

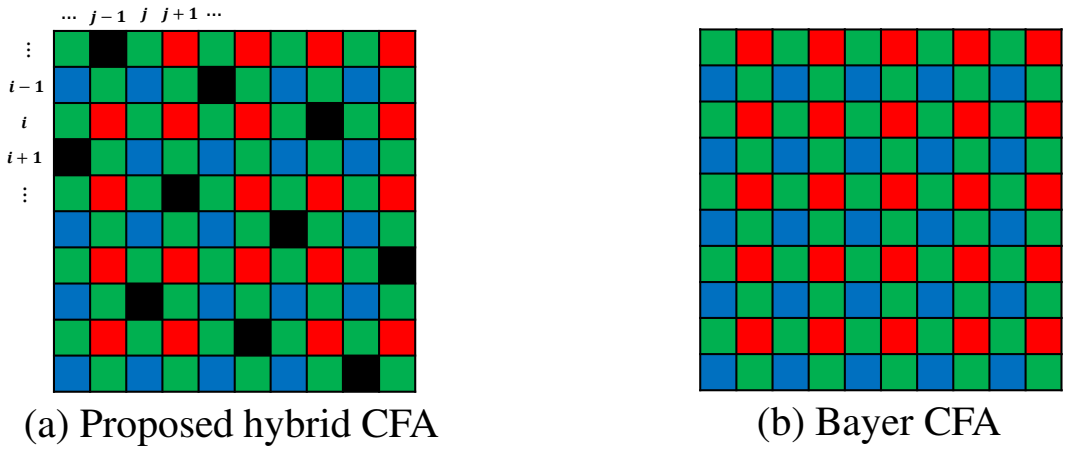

Figure 1. Color filter arrays. The black pixels of the proposed hybrid CFA represent the additional band pixels.

2. HYBRID COLOR FILTER ARRAY

The proposed hybrid CFA is shown in Fig. 1 (a), where the black pixels represent the additional band pixels. We design the hybrid CFA to have the following three desirable properties: (i) The additional band pixels are sampled from the Bayer CFA (Fig. 1 (b)), which is the most popular and widely used CFA.[10] The research on the demosaicking algorithm for the Bayer CFA has a long history and many high-performance algorithms have been proposed. We can easily apply these Bayer demosaicking algorithms for the hybrid CFA by compensating the missing R and B pixel values at the additional band pixel locations. (ii) The sampling density of the G pixels is as high as the Bayer CFA. In the same manner as most of the Bayer demosaicking algorithms, we first interpolate the missing G pixel values, then we exploit inter-channel correlations between G and R or B bands to interpolate the missing R and B pixel values. (iii) The additional band pixels are arrayed on a square grid, while the square grid is slightly slanted. Therefore, we can apply a single-image SR algorithm to interpolate the missing additional band pixel values.

The most simple approach for obtaining the RGB image with the hybrid CFA is to apply the Bayer demosaicking algorithm after interpolating the missing R and B pixel values at the additional band pixel locations. We call this simple approach the naive algorithm. Although the naive algorithm is easy to apply, the performance is insufficient. In the next section, we propose a novel RGB demosaicking algorithm for the hybrid CFA by extending a state-of-the-art Bayer demosaicking algorithm.

3. PROPOSED DEMOSAICKING ALGORITHM

3.1 Overview

Fig. 2 shows the outline of our proposed demosaicking algorithm. We assume that the additional band image is uncorrelated with the RGB image, and independently interpolate the missing RGB and the additional band pixel values.

For the RGB image demosaicking, we first interpolate the missing G pixel values. We propose a novel G pixel value interpolation algorithm for the hybrid CFA by extending the gradient based threshold free (GBTF) algorithm,[11] which is one of the state-of-the-art Bayer demosaicking algorithms. We describe the proposed G pixel value interpolation algorithm in Sec. 3.2. After the G pixel value interpolation, we interpolate the missing R and B pixel values by using the guided filter,[12] which is a recently proposed excellent structure-preserving filter. For each of the local patches, the guided filter interpolates the missing pixel values by a linear transformation of a given guide image. We use the interpolated G band image as the guide image.[13,14]

After once the RGB image is demosaicked, we introduce an iterative framework to improve the RGB demosaicking algorithm. In the iterative framework, we obtain the Bayer mosaic data from the demosaicked RGB image and update the guide image (G band image) by using the Bayer demosaicking algorithm (Fig. (2)). Then,

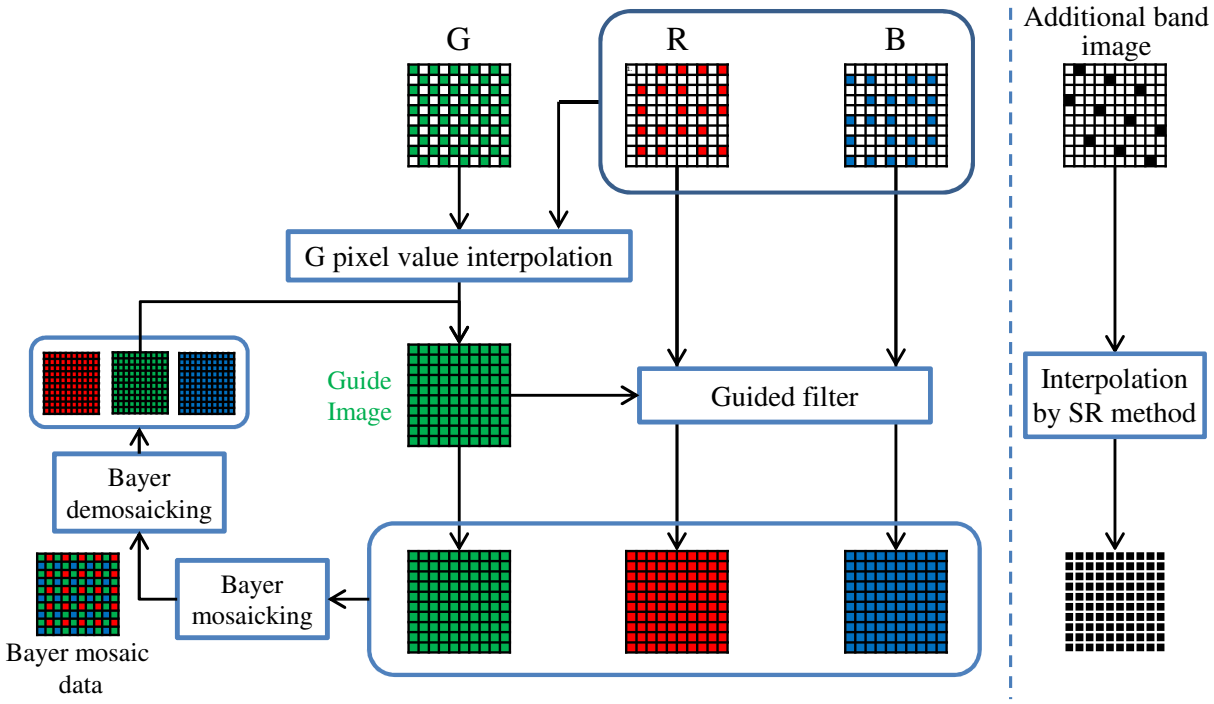

Figure 2. Outline of our proposed demosaicking algorithm.

we interpolate the R and B pixel values by the guided filter using the updated guide image. This iteration framework improves the performance of the RGB image demosaicking.

For the additional band image demosaicking, we apply a single-image SR algorithm. In the proposed hybrid CFA, the additional band pixels are arrayed on a square grid. Although the square grid is slanted, we can apply the single-image SR algorithm by rectifying the additional band pixels to the regular square grid. We use the sparse mixing estimators (SME),[15] which is one of the best single-image SR algorithms, and upsample the additional band pixel values by a scale factor of 4×4. Then, we resample the upsampled pixel values to the original slanted square grid.

3.2 Proposed G pixel value interpolation

We propose a novel G pixel value interpolation algorithm for the hybrid CFA by extending the GBTF algorithm.[11] Fig. 3 (a) shows the flow of the G pixel value interpolation by the GBTF algorithm for the Bayer CFA. The G pixel value interpolation by the GBTF algorithm consists of three steps: (i) The Hamilton and Adams' interpolation formula[16] is applied to all pixels in both horizontal and vertical directions. Then, the horizontal and vertical color differences (G-R or G-B) at each pixel location are calculated (horizontal and vertical filtering and subtracting). (ii) The horizontal and vertical color differences are respectively smoothed out. The smoothed horizontal and vertical color differences are combined into the final color difference estimation at each R or B pixel location. (iii) The R and the B pixel values in the Bayer RGB raw data are added to the final color difference estimations to obtain the estimations of G pixel values. We modify step (i) and (iii) for the proposed hybrid CFA.

Fig. 3 (b) shows the flow of the G pixel value interpolation by our proposed demosaicking algorithm for the hybrid CFA. Since the R and the B pixel values at the additional band pixel locations are missing in the hybrid CFA, we first interpolate these missing pixel values and make the Bayer RGB raw data. In the step (i), the GBTF algorithm calculates the color differences in the horizontal and vertical directions. We also apply the directional linear interpolation for obtaining the R and the B pixel values at the additional band pixel locations

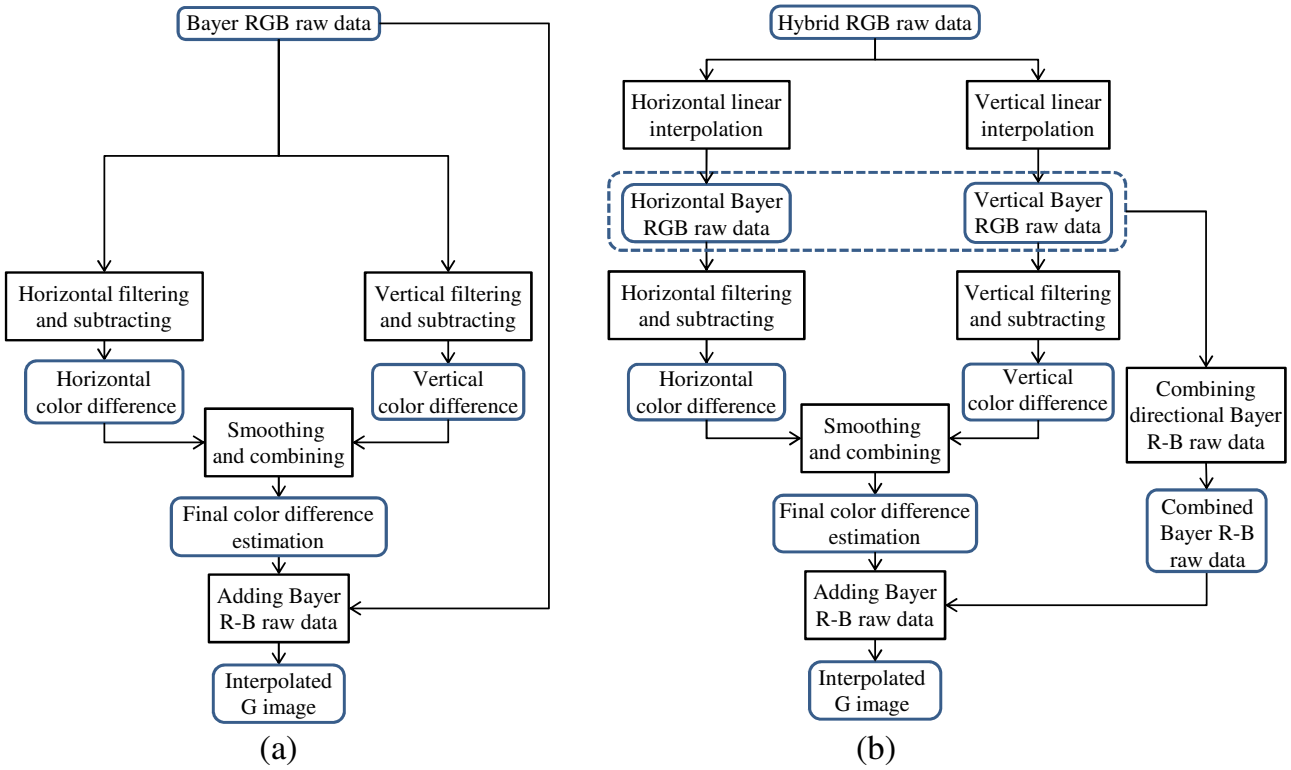

Figure 3. Flow of G pixel value interpolation (a) by the GBTF algorithm for the Bayer CFA, and (b) by the proposed algorithm for the hibrid CFA.

as:

$$\begin{aligned} R^H_{i,j} &= (R_{i,j-2} + R_{i,j+2})/2, \\ R^V_{i,j} &= (R_{i-2,j} + R_{i+2,j})/2, \end{aligned} \tag{1}$$

where the suffix i, j represents the target pixel location, $R^H_{i,j}$ is the horizontally interpolated pixel value, and $R^V_{i,j}$ is the vertically interpolated pixel value. The B pixel values at the additional band pixel locations are similarly interpolated. As the result of this directional interpolation, we obtain both the horizontal and the vertical Bayer RGB raw data. Based on these two directional Bayer RGB raw data, the step (i) is performed. The Hamilton and Adams' interpolation formula[16] is applied to all pixels in both vertical and horizontal directions. For red pixel locations, horizontal green channel estimations are calculated as:

$$\tilde{G}^H_{i,j} = -\tfrac{1}{4}R_{i,j-2} + \tfrac{1}{2}G_{i,j-1} + \tfrac{1}{2}R_{i,j} + \tfrac{1}{2}G_{i,j+1} - \tfrac{1}{4}R_{i,j+2}. \tag{2}$$

For green pixels with red horizontal neighbors, the horizontal red channel estimation is calculated similarly as:

$$\tilde{R}^H_{i,j} = -\tfrac{1}{4}G_{i,j-2} + \tfrac{1}{2}R_{i,j-1} + \tfrac{1}{2}G_{i,j} + \tfrac{1}{2}R_{i,j+1} - \tfrac{1}{4}G_{i,j+2}. \tag{3}$$

The vertical estimations are calculated similarly. The color differences for horizontal and vertical directions are calculated as:

$$\begin{aligned} \tilde{\Delta}^H_{g,r}(i,j) &= \begin{cases} \tilde{G}^H_{i,j} - R_{i,j}, & \text{G is interpolated} \\ G_{i,j} - \tilde{R}^H_{i,j}. & \text{R is interpolated} \end{cases} \\ \tilde{\Delta}^V_{g,r}(i,j) &= \begin{cases} \tilde{G}^V_{i,j} - R_{i,j}, & \text{G is interpolated} \\ G_{i,j} - \tilde{R}^V_{i,j}. & \text{R is interpolated} \end{cases} \end{aligned} \tag{4}$$

The color differences at blue pixels are calculated in the same manner, simply by replacing R with B in the formulas above.

Next, in the step (ii), the directional color differences are smoothed and combined as:

$$\begin{aligned}\tilde{\Delta}_{g,r}(i,j) = \{&\omega_N * f * \tilde{\Delta}^V_{g,r}(i-4:i,j)+\\ &\omega_S * f * \tilde{\Delta}^V_{g,r}(i:i+4,j)+\\ &\omega_E * \tilde{\Delta}^H_{g,r}(i,j-4:j) * f'+\\ &\omega_W * \tilde{\Delta}^H_{g,r}(i,j:j+4) * f'\}/\omega_T,\\ &\omega_T = \omega_N + \omega_S + \omega_E + \omega_W.\end{aligned} \tag{5}$$

In the GBTF[11] algorithm, the simple averaging filter, $f = [11111]/5$, is used for smoothing the directional color differences in Eq. (5). In the proposed algorithm, we apply a Gaussian weighted averaging filter, $f = [0.56, 0.35, 0.08, 0.01, 0]$, instead of the simple averaging filter. We empirically use 1 for the standard deviation of the Gaussian weight. This weighted averaging filter improves the performance. The weight for each direction $(\omega_N, \omega_S, \omega_E, \omega_W)$ is calculated using color difference gradients in horizontal and vertical directions as:

$$\begin{aligned}\omega_E &= 1/\left(\sum_{a=i-2}^{i+2}\sum_{b=j}^{j+4} D^H_{a,b}\right)^2, \qquad \omega_W = 1/\left(\sum_{a=i-2}^{i+2}\sum_{b=j-4}^{j} D^H_{a,b}\right)^2,\\ \omega_N &= 1/\left(\sum_{a=i-4}^{i}\sum_{b=j-2}^{j+2} D^V_{a,b}\right)^2, \quad \omega_S = 1/\left(\sum_{a=i}^{i+4}\sum_{b=j-2}^{j+2} D^V_{a,b}\right)^2,\end{aligned} \tag{6}$$

where the directional gradients $D^H_{i,j}$ and $D^V_{i,j}$ are calculated as:

$$D^H_{i,j} = \|\tilde{\Delta}^H_{i,j-1} - \tilde{\Delta}^H_{i,j+1}\|, \quad D^V_{i,j} = \|\tilde{\Delta}^V_{i-1,j} - \tilde{\Delta}^V_{i+1,j}\|. \tag{7}$$

Finally, in the step (iii), we need to add the R or the B pixel values in Bayer RGB raw data to the final color differences for the estimation of G pixel values. However, in the proposed algorithm, the horizontally and vertically interpolated R and B pixel values at the additional band pixel locations are not unique (Eq. (1)). Therefore, we need to combine the horizontally and vertically interpolated pixel values before applying the step (iii). We follow the similar combining algorithm for directional color differences as Eq. (5). We calculate the combined R pixel value at the additional pixel location as:

$$\hat{R}_{i,j} = \{\omega_H R^H_{i,j} + \omega_V R^V_{i,j}\}/\left(\omega_H + \omega_V\right), \tag{8}$$

where the horizontally and vertically interpolated R pixel values $\left(R^H_{i,j}, R^V_{i,j}\right)$ are calculated by Eq. (1), and the horizontal and vertical weights ω_H, ω_V are calculated as:

$$\omega_H = 1/\left(\sum_{a=i-2}^{i+2}\sum_{b=j-2}^{j+2} D^H_{a,b}\right)^2, \quad \omega_V = 1/\left(\sum_{a=i-2}^{i+2}\sum_{b=j-2}^{j+2} D^V_{a,b}\right)^2. \tag{9}$$

Then, we obtain the final estimation of G pixel values by adding the combined R or B pixel values.

$$\begin{aligned}\tilde{G}(i,j) &= \hat{R}(i,j) + \tilde{\Delta}_{g,r}(i,j),\\ \tilde{G}(i,j) &= \hat{B}(i,j) + \tilde{\Delta}_{g,b}(i,j).\end{aligned} \tag{10}$$

Table 1. Comparison of the average PSNRs of 25 images.

	R	G	B	NIR
Bayer & GBTF[11]	34.30	38.85	35.35	NA
Lu et al.[8]	32.77	34.05	32.80	**35.02**
Sadeghipoor et al.[9]	32.03	33.53	32.32	33.88
Naive	32.06	35.66	33.05	29.48
Proposed	**33.34**	**38.43**	**35.15**	30.10

4. EXPERIMENTS

4.1 Visual and PSNR comparisons

The proposed algorithm is evaluated with 25 RGB and NIR image pairs.[8,9] The size of the image pairs is 768×512. Although our proposed algorithm is not limited to the capturing of the RGB and the NIR images, we use the NIR image as the additional band image in this paper to compare with the existing CFAs and algorithms.[8,9] We compare the proposed algorithm with Lu's algorithm,[8] Sadeghipoor's algorithm,[9] the naive algorithm with the hybrid CFA described in the Sec. 2, and the GBTF algorithm[11] with the Bayer CFA. In the naive algorithm, the RGB images are demosaicked by the GBTF algorithm after bilinear interpolation of R and B pixel values at the additional band pixel locations and the NIR images are demosaicked by bilinear interpolation.

The average PSNRs of the 25 image pairs are shown in Table 1. In terms of the average PSNR of the RGB images, the proposed algorithm outperforms the existing algorithms,[8,9] which can obtain both the RGB and NIR images. Although the GBTF algorithm with the Bayer CFA gives a better performance than the proposed algorithm, the GBTF algorithm with the Bayer CFA can not provide the NIR images. The visual comparison of the RGB images are shown in the top row of Fig. 4 and Fig. 5. As shown in these figures, our proposed algorithm can generate the RGB images with almost the same quality as the RGB images acquired by using the standard Bayer CFA.

For the NIR images, the average PSNR of the proposed algorithm is lower than the existing algorithms.[8,9] The reason is that the existing algorithms assume the strong correlation between the RGB and the NIR images. The bottom row of Fig. 4 shows the NIR images which have strong correlation with the RGB images. In this scene, the existing algorithms can interpolate the NIR images more sharply than the proposed algorithm. However, the assumption of this correlation is not always true. If the assumption of this correlation collapses, the quality of the NIR image is significantly degraded as shown in the bottom row of Fig. 5. The additional band image is uncorrelated with the RGB image in some applications. For such applications, the proposed additional band image demosaicking is expected to outperform the existing algorithms.

4.2 Real scene examples

To show real scene examples, we captured the RGB and NIR image pair and simulated our proposed hybrid CFA and demosaicking algorithm. We used the Canon EOS 7D camera and removed a hot mirror, which is a NIR blocking filter in front of the sensor, to capture the NIR components. By using this modified camera, we sequentially captured the RGB image with the NIR cut filter and the NIR image with the visible-band cut filter. Then, we mosaicked the captured RGB and NIR images for the hybrid CFA and applied our proposed demosaicking algorithm to simulate our proposed hybrid CFA and demosaicking algorithm. We also simulated the Bayer CFA and the GBTF algorithm for the comparison.

The top row of the Fig. 6 shows an example of the captured RGB and NIR image pair, where the NIR dot patterns are projected by using the Microsoft's Kineck. The middle and bottom rows show the originally capured and the simulated RGB and NIR images. As shown in these results, our proposed hybrid CFA and demosaicking algorithm can simultaneously acquire the high-quality RGB image and the effective additional band image, in which the NIR dot patterns are visible.

Figure 4. Visual comparison of the RGB and NIR images of the roof.

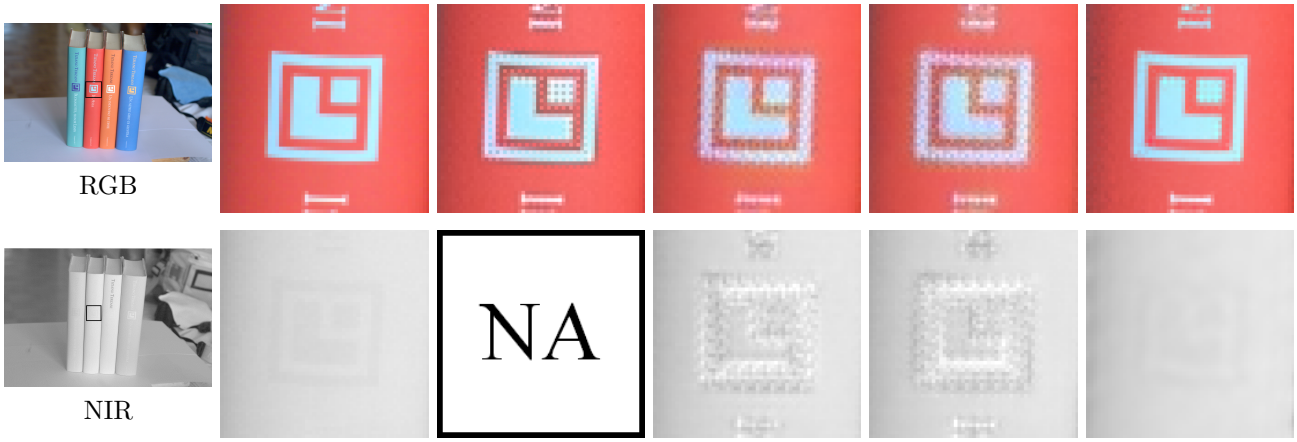

Figure 5. Visual comparison of the RGB and NIR images of the book.

5. CONCLUSION

In this paper, we have proposed the novel hybrid CFA and the demosaicking algorithm for the simultaneous capturing of the RGB and the additional band images. Unlike existing algorithms, our proposed hybrid CFA and demosaicking algorithm do not rely on any specific correlation between the RGB and the additional bands to acquire the independent information derived from the additional band image. Experimental results demonstrate that our proposed hybrid CFA and demosaicking algorithm can provide the additional band image while keeping the RGB image with almost the same quality as the image acquired by using the Bayer CFA.

REFERENCES

[1] Li, S. Z., Chu, R. F., Liao, S. C., and Zhang, L., "Illumination invariant face recognition using near-infrared images," *IEEE Trans. on Pattern Analysis and Machine Intelligence* **29**(4), 627–639 (2007).

[2] Hamamoto, Y., Endo, T., Nosho, K., Arimura, Y., Sato, M., and Imai, K., "Usefulness of narrow-band imaging endoscopy for diagnosis of barretts esophagus," *Journal of gastroenterology* **39**(1), 14–20 (2004).

[3] Hao, Y., Sun, Z., and Tan, T., "Comparative studies on multispectral palm image fusion for biometrics," *Proc. of Asian Conf. on Computer Vision (ACCV)* , 12–21 (2007).

[4] Krishnan, D. and Fergus, R., "Dark flash photography," *ACM Trans. on Graphics* **28(3)**(96) (2009).

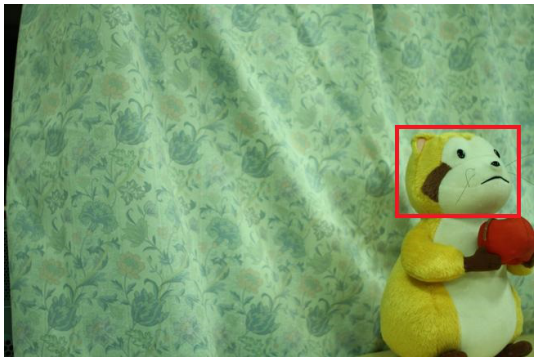

RGB

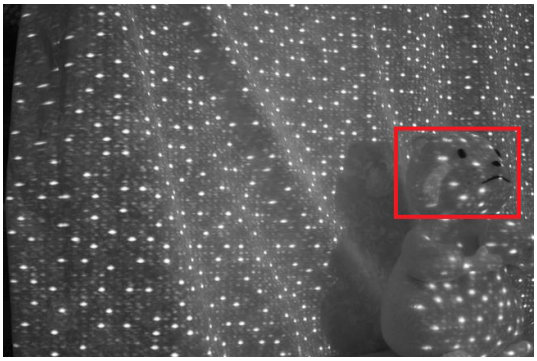

NIR

Original RGB image

Bayer & GBTF RGB image

Proposed RGB image

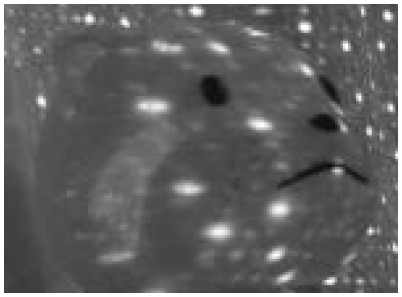

Original NIR image

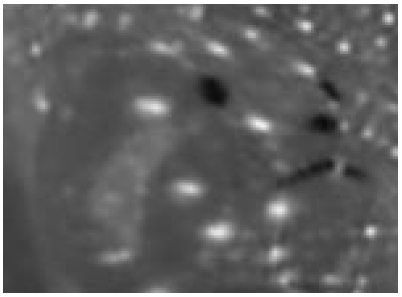

Proposed NIR image

Figure 6. Visual comparison of the real scene example.

[5] Süsstrunk, S. and Fredembach, C., "Enhancing the visible with the invisible: Exploiting near-infrared to advance computational photography and computer vision," *SID International Symposium Digest* **41**(1), 90–93 (2010).

[6] Zhang, X., Sim, T., and Miao, X., "Enhancing photographs with near infra-red images," *Proc. of the Conf. on Computer Vision and Pattern Recognition (CVPR)* , 1–8 (2008).

[7] Lukac, R., [*Single-sensor imaging: methods and applications for digital cameras*], CRC Press (2008).

[8] Lu, Y. M., Fredembach, C., Vetterli, M., and Süsstrunk, S., "Designing color filter arrays for the joint capture of visible and near-infrared images," *Proc. of IEEE Int. Conf. on Image Processing (ICIP)* , 3797–3800 (2009).

[9] Sadeghipoor, Z., Lu, Y. M., and Süsstrunk, S., "Correlation-based joint acquisition and demosaicing of visible and near-infrared images," *Proc. of IEEE Int. Conf. on Image Processing (ICIP)* , 3226–3229 (2011).

[10] Bayer, B., "Color imaging array," *U.S. Patent 3971065* (1976).

[11] Pekkucuksen, I. and Altunbasak, Y., "Gradient based threshold free color filter array interpolation," *Proc. of IEEE Int. Conf. on Image Processing (ICIP)* , 137–140 (2010).

[12] He, K., Sun, J., and Tang, X., "Guided image filtering," *Proc. of the 11th European Conf. on Computer Vision (ECCV)* **6311**, 1–14 (2010).

[13] Monno, Y., Tanaka, M., and Okutomi, M., "Multispectral demosaicking using adaptive kernel upsampling," *Proc. of IEEE Int. Conf. on Image Processing (ICIP)* , 3218–3221 (2011).

[14] Monno, Y., Tanaka, M., and Okutomi, M., "Multispectral demosaicking using guided filter," *Proc. of SPIE* **8299**, 82990O–1–82990O–7 (2012).

[15] Mallat, S. and Yu, G., "Super-resolution with sparse mixing estimators," *IEEE Trans. on Image Processing* **19**(11), 2889–2900 (2010).

[16] Hamilton Jr, J. and Adams Jr, J., "Adaptive color plan interpolation in single sensor color electronic camera," (1997). US Patent 5,629,734.